Hindawi
Journal of Chemistry
Volume 2022, Article ID 4874502, 11 pages
https://doi.org/10.1155/2022/4874502

Research Article

The Application of the Activated Carbon from *Cordia africana* Leaves for Adsorption of Chromium (III) from an Aqueous Solution

Estifanos Kassahun,[1] Jemal Fito,[2] Solomon Tibebu,[3] Thabo T. I. Nkambule,[2] Talebachew Tadesse,[4] Takele Sime,[3] and Helmut Kloos[5]

[1]*Food and Beverage Industry Research and Development Center, Addis Ababa, Ethiopia*
[2]*Institute for Nanotechnology and Water Sustainability (iNanoWS), College of Science Engineering and Technology, University of South Africa, Florida Science Campus, Johannesburg 1710, South Africa*
[3]*Department of Environmental Engineering, College of Biological and Chemical Engineering, Sustainable Energy Center of Excellence, Bioprocess and Biotechnology Center of Excellence, Addis Ababa Science and Technology University, Addis Ababa 16417, Ethiopia*
[4]*Kombolcha Institute of Technology, Wollo University, Dessie, Ethiopia*
[5]*Department of Epidemiology and Biostatistics, University of California, San Francisco, USA*

Correspondence should be addressed to Jemal Fito; fitojemal120@gmail.com

Received 18 October 2022; Revised 15 November 2022; Accepted 18 November 2022; Published 24 November 2022

Academic Editor: Doina Humelnicu

The objective of this study is to investigate the adsorption performance of activated carbon derived from the leaves of *Cordia africana* for the removal of Cr (III) from an aqueous solution. The plant sample was collected, washed, dried, grounded, and sieved at 125 μm mesh size. Adsorbent activation was done using H_3PO_4 at concentrations of 25–85% and pyrolysis temperature of 400–500°C. The activated carbon was characterized by proximate, SEM, BET, and FTIR analyses. A batch adsorption study was conducted to determine the effect of contact time, adsorbent dose, initial chromium concentration, and mixing speed on Cr (III) removal. The regeneration of the activated carbon was investigated by using 1 M of HNO_3 as a desorbing solution for seven cycles. At optimum acid concentration and pyrolysis temperature, a surface area of 700 m^2/g was recorded. The moisture content, volatile matter, ash composition, fixed carbon, and bulk density of the activated carbon were found to be 5.3%, 24.2%, 6.2%, 64.3%, and 0.75 g/mL, respectively. The SEM and FTIR analyses indicated that the surface morphology was full of cracks and different peaks were associated with plenty of functional groups, respectively. The maximum Cr (III) removal was attained at a contact time of 180 min (89%), adsorbent dose of 1.5 g (54%), initial concentration of 0.6 g/L (47%), and mixing speed of 300 rpm (64%). The equilibrium data were better described by Freundlich isotherm at R^2 value of 0.88, which implies that the adsorption process is conducted on a heterogeneous surface. The pseudo-first-order kinetics model with R^2 value of 0.99 best fits with the equilibrium data, which implies that physisorption controls the adsorption kinetics. Generally, it can be concluded that this locally prepared adsorbent is promising for the removal of chromium from industrial wastewater, but further factorial approach assessment has to be checked.

1. Introduction

Rapid population growth, industrialization, extensive agriculture, and urbanization are the common reasons for the degradation of environmental quality, especially in developing countries including Ethiopia [1]. Moreover, the growth of water-intensive industries is causing stress on freshwater availability [2]. On the other hand, the contamination of water bodies by industrial effluents is becoming a big problem [3]. Industrial effluents mainly

contain heavy metals, organic matter, and inorganic matter [4]. Tannery industries release effluent which contains a high concentration of heavy metals especially chromium ions into the environment [5]. Discharging tannery effluents into rivers without treatment can cause a major problem for the environment and the community who live near the tannery industries and downstream of the rivers [6]. Chromium ions damage different organs including the liver, kidney, and lung. It can also cause cancer and denature DNA. Generally, chromium pollution can affect both terrestrial and aquatic environments including soil, algae, fishes, and other living and non-living components of the environment [5]. Therefore, chromium remediation from wastewater is essential to prevent environmental pollution.

Conventional wastewater treatment technologies such as preliminary, primary, and secondary treatment units have been used for years. However, these units can only remove suspended solids, dissolved solids, organic matter, and nutrients. Micro-pollutants including heavy metals cannot be efficiently removed by conventional wastewater treatment technologies. Heavy metals were removed effectively by advanced wastewater treatment technologies but were not removed completely [7]. Such treatment technologies are ion exchange, electrodialysis, reverse osmosis, and membrane technologies (micro-filter, nano-filter, and ultra-filter). However, these treatment technologies are very expensive in terms of energy, chemical, and operational cost. However, adsorption is the most promising technology among advanced treatment technologies in terms of cost and treatment efficiency. Adsorption has a high potential to remove micro-pollutants including heavy metals [8, 9]. Especially commercial activated carbons are effective in removing different pollutants from water and wastewater, but they are not widely used because of their high cost [10, 11]. However, locally prepared activated carbons are widely used as adsorbents due to their high potential in removing different pollutants. Moreover, locally prepared activated carbons are low-cost, easy to prepare, highly efficient, and environmentally friendly materials [12, 13]. But, the application of this technology is still at the early stage to scale up at the industrial level [14, 15]. Therefore, searching for efficient and effective adsorbents, which are locally available, is still under investigation.

Activated carbons prepared from biomass residues were found to be a good adsorbent for the removal of chromium ions from wastewater [16, 17]. Currently, many industries are using commercial activated carbons for the remediation of their wastewater. However, many researchers are striving for the replacement of commercial activated carbons with locally prepared biomasses including the leaves of trees and crops [18]. *Cordia africana* is an African tree, which is commonly known as Wanza in Ethiopia. It is a pioneer tree that grows naturally throughout sub-Saharan Africa and tropical Arabia. In Ethiopia, *Cordia africana* is an indigenous tree that is found in different parts of the country. It grows in areas with altitudes between 550 and 2600 m above sea level. The stem of *Cordia africana* is used for timber production, and its fruits are edible and eaten in many parts of Ethiopia. *Cordia africana* is used as a shade tree in coffee cultivation. The fallen leaves are used as mulch and play a great role in nutrient recycling. *Cordia africana* supplies abundant pollen and copious nectar to the bees [19].

Adsorption of Cr (III) from aqueous solutions using different materials has been studied extensively. Alemu et al. [2] reported Cr (III) removal efficiency of 55% using vesicular basalt rock as an adsorbent. A 92% Cr (III) removal efficiency was achieved by using a modified bio-sorbent derived from *Artocarpus nobilis* [20]. However, it is noted that the preparation of activated carbon from fallen leaves of *Cordia africana* and adsorption of Cr (III) using *Cordia africana*-based activated carbon has not been investigated yet. In addition, the study used chromium sulfate as a source of Cr (III), which is a direct chemical compound being used in many leather industries in Ethiopia. Therefore, the objective of this study is to investigate the adsorption performance of the activated carbon derived from the leaves of *Cordia africana* for the removal of Cr (III) from an aqueous solution. Different adsorption factors (contact time, adsorbent dose, initial Cr (III) concentration, and mixing speed), adsorption isotherm, adsorption kinetics, and regeneration of the adsorbent were studied in this investigation.

2. Materials and Methods

2.1. Adsorbent Preparation. The leaves of *Cordia africana* were collected from the premises of Addis Ababa Science and Technology University, Ethiopia. A sufficient amount of leave sample was washed with distilled water several times to remove the impurities. The well-washed samples were dried in an oven (Model BOV-T50F) at 105°C for 24 h to remove the moisture [21]. The dried samples were then grounded by a high-speed multi-function miller (Model HC-700) and sieved by 125 μm mesh size. The sample was ready for carbonation and activation processes. Table 1 depicts the activation process of *Cordia africana* leaves under variable activation temperatures (400–500°C) and acid concentrations (25–85%) [22]. This optimization process was intended to produce high biochar yields and specific surface area.

About 30 g of powdered leaves was impregnated with H_3PO_4 (85% w/w, Merck) at the ratio of 1 : 1 with different acid concentrations (25%, 55%, and 85%) for 24 h and heated in an oven at 60°C [23]. This impregnation ratio was taken constantly throughout the experiment. The impregnated precursors were carbonized in a muffle furnace (Model Nabertherm F 330) at different temperatures (400, 450, and 500°C) at a heating rate of 25°C/min for 1 h [16]. This carbonized activated carbon was washed several times with a total of 2 L distilled water until the supernatant pH becomes 7. Then, the activated carbon was dried in an oven for 24 h at 70°C. Finally, the activated carbon was placed in an airtight plastic container for use [24].

2.2. Adsorbent Characterization. The proximate analysis (moisture content, volatile matter, ash, and fixed carbon) for the optimized activated carbon was determined according to the American Society for Testing and Materials (ASTM

Table 1: Different activating temperatures and acid concentrations for the preparation of activated carbon.

Run	Activation temperature (°C)	Acid concentration (%)
1	400	85
2	400	55
3	400	25
4	450	85
5	450	55
6	450	25
7	500	85
8	500	55
9	500	25

D2866-2869). The carbon yield and bulk density were calculated using equations (1) and (2), respectively

$$\text{Carbon yield} = \frac{\text{mass of activated carbon}}{\text{mass of thedry sample}} * 100, \quad (1)$$

$$\text{bulk density} = \frac{\text{sample mass (gm)}}{\text{sample volume}\left(\text{cm}^3\right)} \text{x } 100. \quad (2)$$

The morphological structures were studied using a scanning electron microscope (SEM, INSPECT-F50) at different resolutions. Standard operating procedures were followed during sample preparation and scanning [25]. The surface area of the activated carbon was measured using a BET surface area analyzer (Horiba, SA-9600). This measurement was operated by taking 0.4 g of activated carbon in three sample tubes at 100°C for 2 h under vacuum conditions. Helium, a non-adsorbable gas, was used to prepare the sample. The adsorption and desorption of nitrogen gas at atmospheric pressure of 700 mm were used by the surface analyzer. The functional groups of the adsorbent were studied using a Fourier transform infrared spectrometer (FTIR, ThermoNicolet 5700) within the spectral range of 4000-400 cm^{-1}. To get a clear pick value in the FTIR graph, the sample to KBr ratio of 1 : 100 was mixed and the analysis was performed [10].

2.3. Batch Adsorption Experiment. The chromium aqueous solution was prepared by dissolving 1.0 g of $Cr_2(SO_4)_3$ (powder, technical grade) into 1 L of distilled water to get a 1000 mg/L concentration. Appropriate dilutions have been made to this aqueous solution to get the needed concentrations. In the batch adsorption experiment, contact time, adsorbent dose, initial Cr (III) concentration, and mixing speed were used as independent variables, whereas the removal efficiency was the response variable. The pH of the solution was fixed at 3 throughout the experiments [26]. About 24 experiments have been carried out for batch adsorption studies. In all experiments, about 200 mL solution was prepared in a 300 mL borosilicate glass stopper reagent bottle at room temperature (25 ± 1°C). Each adsorption factor such as contact time, initial Cr (III) concentration, adsorbent dose, and mixing speed was varied while keeping the other factors constant at 120 min, 0.6 g/L, 0.8 g, and 200 rpm, respectively, as depicted in Table 2.

After the adsorption process, the solution was filtered using grade 42 Whatman filter paper and the concentration of Cr (III) was determined using a UV-visible spectrophotometer (JASCO V-770) at 540 nm wavelength [4].

The removal efficiency of Cr (III) from an aqueous solution was calculated using the following equation:

$$R\% = \frac{C_0 - C_e}{C_0} x100, \quad (3)$$

where R% is the removal efficiency, Co is the initial Cr (III) concentration (mg/L), and Ce is the final Cr (III) concentration (mg/L).

2.4. Adsorption Isotherm. Equilibrium isotherms were studied by dissolving 0.3, 0.4, 0.5, 0.6, 0.7, 0.8, 0.9, and 1 g of chromium into 1 L of solution and placing it into a 300 mL glass bottle. The pH of the solution was adjusted to 3. The value of the factors such as contact time, adsorbent dose, and mixing speed that gives maximum Cr (III) removal were taken constantly for each adsorption isotherm experiment. Each solution was stirred at room temperature 25 ± 1°C. The equilibrium data were fitted with Langmuir and Freundlich isotherms. Langmuir isotherm assumes that maximum adsorption occurs when the adsorbent surface is covered by a single adsorbate layer, whereas the Freundlich model described the multi-layer adsorption of adsorbate [27]. Langmuir and Freundlich's isotherm models are described by equations (4) and (6)

$$\frac{ce}{qe} = \left(\frac{c_e}{q_m}\right) + \frac{1}{q_{\max} k_i}, \quad (4)$$

$$q_e = \frac{C_0 - C_e}{m} x\, V, \quad (5)$$

$$\log q_e = \log K_f + \frac{1}{n} \log Ce, \quad (6)$$

where q_e is the adsorption capacity (mg/g), V is the adsorbate volume (L), m is the mass of adsorbent (g), q_m is the maximum adsorption capacity of (Cr III) adsorbed per unit mass of activated carbon (mg/g), Kl is the Langmuir constant which is related to equilibrium adsorption constant (L/g), K_f is the Freundlich isotherm constant (mg/g), and n is the adsorption intensity. Moreover, the dimensionless constant parameter which is called separation constant (R_L) was determined using the following equation:

$$R_L = \frac{1}{1 + KlC_e}. \quad (7)$$

2.5. Adsorption Kinetics. Adsorption kinetic parameters were determined following the pseudo-first order and pseudo-second order. In the present study, the adsorption kinetics was performed at 60, 120, 180, 240, 300, and 360 min periods. A concentration of 0.6 g/L was put into a 300 mL glass bottle, and the pH of the solution was adjusted to 3.

Table 2: The values of different factors of the adsorption experimental conditions.

Factor	Contact time (min)	Adsorbent dose (g)	Initial Cr (III) concentration (g/L)	Mixing speed (rpm)
1	30, 60, 90, 120, 150, 180, 210, and 240	0.8	0.6	200
2	120	0.5, 0.6, 0.7, 0.8, 1, 1.3, 1.4, 1.5	0.6	200
3	120	0.8	0.3, 0.4, 0.5, 0.6, 0.7, 0.8, 0.9, 1	200
4	120	0.8	0.6	100, 150, 175, 200, 225, 250, 275, 300

The pseudo-first-order and pseudo-second-order models were developed based on solid adsorption capacity expressed as follows, respectively.

$$\log(q - q_t) = \log qe + \frac{K1t}{2.303}, \qquad \frac{t}{qt} = \left(\frac{t}{qe}\right) + \frac{1}{K_{2q_e^2}}, \tag{8}$$

where q_t is the amount of Cr (III) on the surface of the activated carbon at time t (mg·g^{-1}), K_2 is the rate constant of the pseudo-second-order adsorption (g/mg min), and k_1 is the equilibrium rate constant of the pseudo-first-order adsorption (min^{-1}).

2.6. Regeneration Study. Regeneration and reusability of *Cordia africana*-based adsorbent material were investigated by using 1 M of HNO_3 as a desorbing solution. The tests were done by employing 2 g of saturated adsorbent in 150 mL of HNO_3 and agitating it at 400 rpm at 25℃ by mechanical stirrer for 120 min. Then, the regenerated activated carbon was separated from the desorbing solution using filter paper.

A 200 mL solution containing 0.6 g/L of Cr (III) ions concentration was prepared. A 0.8 g of regenerated activated carbon sample was added in to the solution. After mixing the solution for 120 min at 200 rpm, the solution was filtered and the concentration of Cr (III) ions concentration in the solution was checked. The adsorbent material was then washed with ethanol and dried at room temperature. The adsorbent was reprocessed/recycled for cation adsorption for seven successive cycles.

3. Results and Discussion

3.1. Optimization of Activated Carbon Preparation. The preparation of activated carbon derived from the leaves of *Cordia africana* was optimized by investigating the best combination of activation temperature and acid concentration that gives a relatively high yield and surface area. As depicted in Table 3, an activation temperature of 500°C and acid concentration of 85% give an activated carbon with a relatively high yield of 67% and a surface area of 700 m^2/g. The value of the surface area reported by Veeramani et al. [28] in studying activated carbon derived from pumpkin stems is also in agreement with the value reported in this study. The optimized combination that gives a relatively high yield and surface area was used for characterizing the activated carbon, conducting batch adsorption experiments, and studying the adsorption isotherm.

As depicted in Table 3, at constant activation temperature, both surface area and carbon yield increased as the acid concentration increased from 25% to 85%. The increment of the surface area might be due to the attack on the cellulosic and lignocellulose composition of biomass [29]. The increment in yield might be due to the ability of H_3PO_4 to retain carbon and minimize the loss of volatile matter. The promotion of H_3PO_4 to convert aliphatic to aromatic compounds might also play a role in increasing the yield [30]. This condition is true for all activation temperatures (400, 450, and 500°C). At constant acid concentration, as activation temperature increases from 400 to 500°C, the yield first decreases and then increases. Similar result was obtained in other studies [31]. The decrease in yield as activation temperature increases might be due to the promotion of carbon burn-off and tar volatilization, and at relatively high activation temperatures, a slight increment of yield was observed. At constant acid concentration, as activation temperature increases from 400 to 500°C, the surface area first increases and then decreases. This result is in agreement with the previous study [32]. This condition is true for all acid concentrations (85, 55, and 25%).

3.2. Characteristics of the Adsorbent

3.2.1. Proximate Analysis. The moisture content, volatile matter, ash, fixed carbon, and bulk density of the optimized activated carbon were 5, 24, 6, 64%, and 0.74 g/mL, respectively, as depicted in Table 4. Activated carbon that has a low percentage of ash content, moisture content, and high percentage of fixed carbon is considered ideal.

It can be noted that the activated carbon has a low moisture content, low ash content, and high fixed carbon. This might be due to the thermal and acid activation process, which breaks the bonds of the molecules and increases the carbon content [1].

3.2.2. Scanning Electron Microscope (SEM). SEM analysis was used to study the surface structure of *Cordia africana* before and after activation as depicted in Figure 1. A surface magnification of 200 μm was used for both cases. Relative to the surface structure of *Cordia africana* before activation, it was observed that more pore openings are created on the surface structure of *Cordia africana* after activation. This

Table 3: Optimization of the preparation of activated carbon.

Run	Activation temperature (°C)	Acid concentration (%)	Carbon yield (%)	Surface area (m^2/g)
1	400	85	63.3	580
2	400	55	61.6	500
3	400	25	61.0	400
4	450	85	60.3	640
5	450	55	60.0	570
6	450	25	56.6	490
7	500	85	66.6	700
8	500	55	61.6	610
9	500	25	58.3	540

Table 4: Proximate analysis of the AC.

Parameters	Values
Moisture content (%)	5.3
Volatile matter (%)	24.2
Ash content (%)	6.2
Fixed carbon (%)	64.3
Bulk density (g/mL)	0.74

increases the surface area of the activated carbon, which in turn increases the binding sites for the adsorbent. On the micrograph image, the dark structure indicates the passage of electrons through the created pores. The increase of pores on the activated carbon might be resulted due to the elimination of impurities using both chemical activation by phosphoric acid and thermal activation [21].

3.2.3. Fourier Transform Infrared Spectrophotometer (FTIR). The functional groups before activation, after activation, and after adsorption of *Cordia africana* were identified using FTIR spectra. The presence of various functional groups is indicated by the observed different peaks, which in turn indicate the complex nature of the adsorbent [33].

As depicted in Figure 2, the peaks observed at a wavelength of 3294 cm^{-1} correspond to hydroxyl (-OH) stretching vibration [34]. The 2990 cm^{-1} and 2917 cm^{-1} wavelengths correspond to -C-H stretching vibrations in the alkane functional group [35]. At wavelengths of 1716 cm^{-1} and 1770 cm^{-1}, there is C=O stretch vibration. The peaks observed at 1620 cm^{-1}, 1597 cm^{-1}, and 1543 cm^{-1} were attributed to N-H stretch vibration. 1483 cm^{-1}, 1417 cm^{-1}, and 1405 cm^{-1} wavelengths correspond to C=C ring stretching. In 1046 cm^{-1}, 1022 cm^{-1}, and 1040 cm^{-1} wavelengths, there is C-O stretch vibration [36]. The peaks observed at 855 cm^{-1}, 879 cm^{-1}, and 873 cm^{-1} correspond to C-H bending vibration [37]. Additionally, 546 cm^{-1} and 559 cm^{-1} indicated the phosphate groups from the phosphoric acid. It can be noted that the wavelength shift of the precursor between before activation, after activation, and after adsorption indicates that functional groups such as N-H, C=C, C-O, and C-H participated in the adsorption of Cr (III) ions. Chelate structures may be formed as a result of chromium ion adsorption with the functional groups of the activated carbon. The shift of wave numbers between before activation and after activation might be due to the increase of surface area due to thermal and chemical activation. The wavenumber shift between after activation and after adsorption might be due to the adsorption of Cr (III) ions on the surface of the adsorbent [38].

3.3. Effect of Contact Time. The effect of contact time on Cr (III) removal was studied by varying the contact time from 30 min to 240 min while keeping the adsorbent dose, initial Cr (III) concentration, and mixing speed constant at 0.8 g, 0.6 g/L, and 225 rpm, respectively. The Cr (III) removal efficiency rapidly increased from 32% to 69% when contact time increased from 30 min to 90 min. This might be due to the availability of a large surface area on the adsorbent surface at the beginning of adsorption. The removal efficiency then relatively slowly increased from 69% to 86% as contact time increased from 90 min to 240 min. This might be due to the decrease of available surface area on the adsorbent surface as contact time progresses [39]. Moreover, the removal efficiency will not significantly increase after the adsorption process reaches a steady state [40]. The adsorption process slows down at a later phase of adsorption due to the repulsion between bulk liquid and solute molecules. The maximum Cr (III) removal efficiency (89%) was attained at a contact time of 180 min as depicted in Figure 3.

3.4. Effect of Adsorbent Dose. The effect of adsorbent dose on Cr (III) removal efficiency was studied by varying the adsorbent dose from 0.5 to 1.5 g while keeping contact time, initial concentration, and mixing speed constant at 120 min, 0.6 g/L, and 225 rpm, respectively. The Cr (III) removal efficiency increased from 34 to 54% as the adsorbent dose increased from 0.5 to 1.5 g. This might be due to the increase in the surface area of the adsorbent, which in turn increases the number of available binding sites for the adsorption process [41]. At a lower adsorbent dose, the adsorption sites are insufficient and the adsorption sites increase as the adsorbent dose increases. Yusuff [42] also reported an increase in the removal efficiency of Hexavalent Chromium as the adsorbent dose increased from 0.4 to 1 g. The maximum Cr (III) removal efficiency (54%) was attained at an adsorbent dose of 1.5 g as depicted in Figure 4.

3.5. Effect of Initial Concentration. The initial concentration of Cr (III) was varied from 0.3 to 1 g/L to study the effect of initial Cr (III) concentration on Cr (III) removal efficiency as

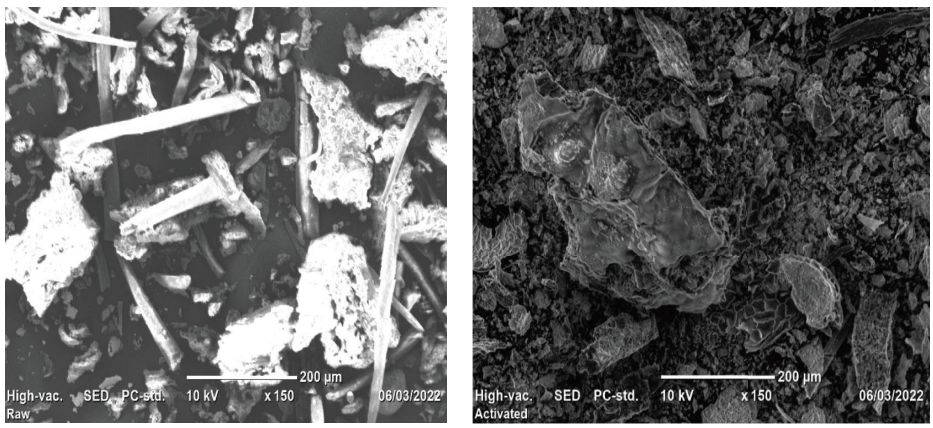

(a) (b)

Figure 1: SEM image of *Cordia africana* before activation (a) and after activation (b).

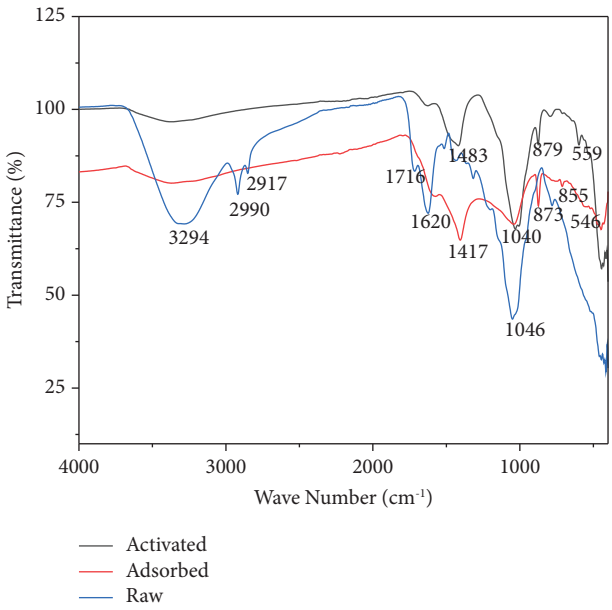

Figure 2: Some important peaks from FTIR analysis for raw precursor-activated carbon before adsorption and after adsorption.

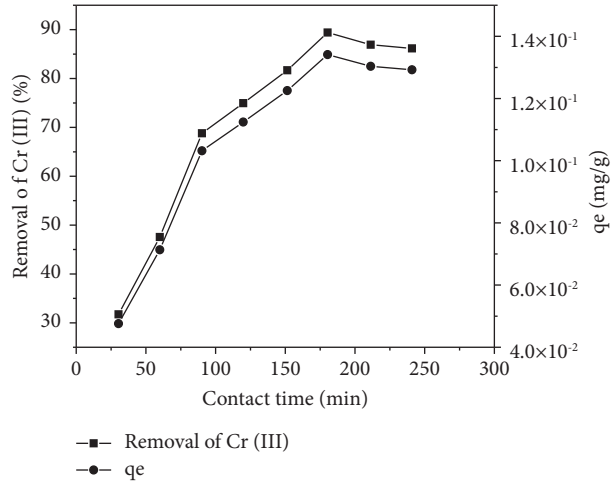

Figure 3: Effect of contact time on Cr (III) removal.

depicted in Figure 5. The experiment was carried out at constant contact time (120 min), adsorbent dose (0.8 g), and mixing speed (225 rpm). The Cr (III) removal efficiency increased from 36 to 46.7% as the initial Cr (III) concentration increased from 0.3 g/L to 0.6 g/L. This might be due to the provision of the driving force that overcomes the mass transfer resistance between the surfaces of the adsorbent and adsorbate molecules. The Cr (III) removal efficiency decreased from 47 to 38% as the initial Cr (III) concentration increased from 0.6 to 1 g/L. This might be due to the saturation of active sites of the adsorbent by the adsorbates (Cr (III) ions) [43]. The maximum Cr (III) removal efficiency (47%) was attained at an initial Cr (III) concentration of 0.6 g/L.

3.6. Effect of Mixing Speed. The effect of mixing speed on Cr (III) removal efficiency was studied by varying the mixing speed from 100 rpm to 300 rpm while keeping the initial Cr (III) concentration, adsorbent dose, and mixing speed constant at 0.6 g/L, 0.8 g, and 225 rpm, respectively, as depicted in Figure 6. The Cr (III) removal efficiency slightly increased from 63 to 64% as the mixing speed increased from 100 to 300 rpm. This might be due to the increase of turbulence in the mixing zone evenly spreading the adsorbents and adsorbates, which will increase the effectiveness of the adsorbent [44]. The maximum Cr (III) removal efficiency (64%) was attained at a mixing speed of 300 rpm.

3.7. Adsorption Isotherm. Langmuir and Freundlich are the two most commonly used isotherm models. The Langmuir isotherm is a concept of the adsorption leading to a monolayer without interaction among the adsorbate

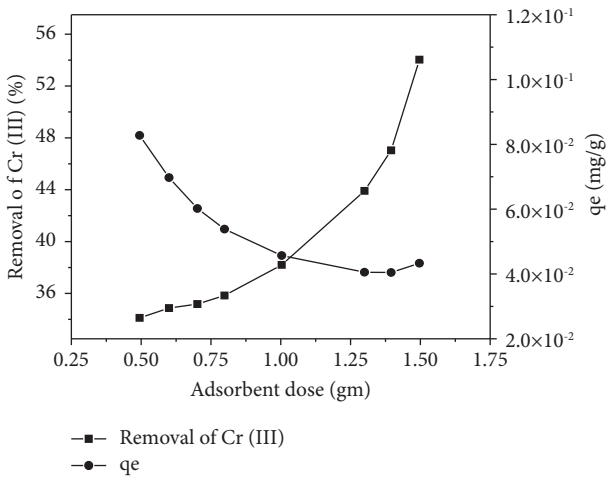

Figure 4: Effect of adsorbent dose on Cr (III) removal.

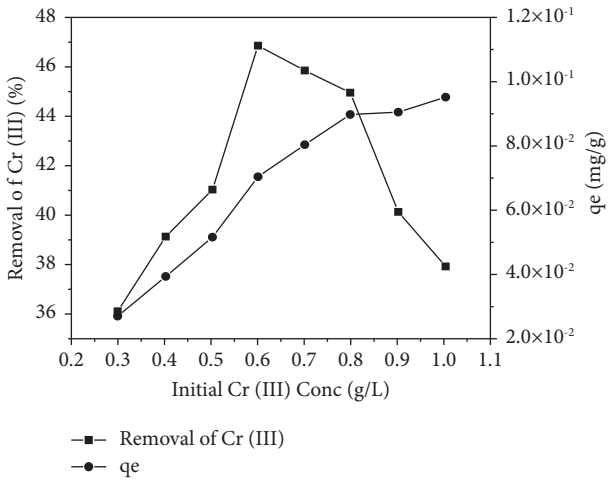

Figure 5: Effect of initial Cr (III) concentration on Cr (III) removal.

molecules. The adsorption takes place at specific sites within the adsorbent. The R^2 value, which is the indicative of the actual deviation between the experimental points for Langmuir isotherm, was found to be 0.87. The values of Q_m and K_m were determined for the adsorbent from the intercept and slopes of the linear plots. The values were 0.011 mg/g and 7.82 L/g, respectively.

Freundlich isotherm models indicate that the adsorption process is conducted on a heterogeneous surface and adsorption capacity is related to the concentration of the adsorbent [45]. K_f indicates adsorption capacity and $1/n$ measures adsorption intensity. The linear isotherm correlation coefficients (R^2) indicate that the equilibrium data are better described by the Freundlich isotherm with an R^2 value of 0.88 as depicted in Table 5. The K_f and $1/n$ values obtained in this study were 0.37 and 0.92, respectively, as depicted in Table 5. The value for $1/n$ for the activated carbon is less than 1, which indicates normal and favorable adsorption and more heterogeneous surfaces with more functional groups that favor the adsorption.

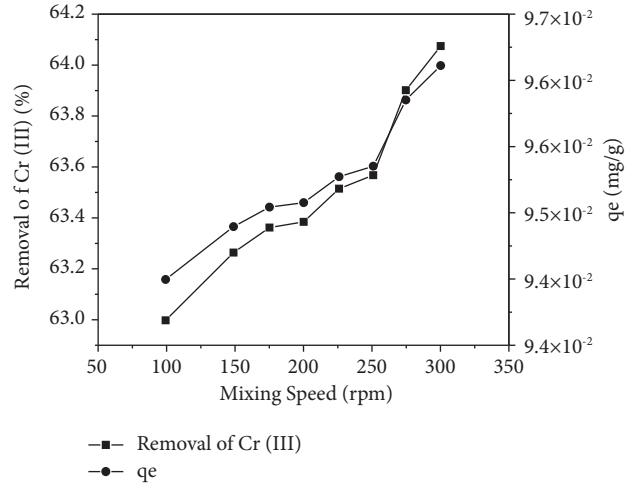

Figure 6: Effect of mixing speed on Cr (III) removal.

3.8. Adsorption Kinetics. Kinetic studies evaluated the details of the process whereby a system moves from an initial state to the final state and the time required for this transition. In this study, the relative slopes and intercepts of a plot of log $(q_e - q_t)$ and t/q_t versus t have been used to compute q_e, the first-order rate constant K_1, and second-order rate constant K_2. The linear plot of the kinetics models for Cr (III) adsorption onto the activated carbon is depicted in Table 6. The best-fitting model was chosen based on the linear correlation coefficient (R^2). The equilibrium data best fit with the pseudo-first-order model with an R^2 value of 0.99. This indicates that physisorption controls the adsorption kinetics [46]. The K_1, K_2, q_{e1}, and q_{e2} values obtained in this study were 3.85, 2.94×10^{-4}, $10^{-7.81}$, and 54.65, respectively.

This research is compared with other research studies that were conducted on chromium removal by activated carbon in terms of maximum adsorption capacity (Qe max) and BET surface area as depicted in Table 7.

3.9. Regeneration Study. As depicted in Figure 7, the removal efficiency of the adsorbent for seven cycles decreased from 86% to 17%. The adsorption efficiency of reused adsorbent dropped by about 14% and 15% in the first and second cycles, respectively. The regeneration process involves the exchange of proton between HNO_3 and cation-adsorbed activated carbon in the repeated adsorption-desorption cycles. The adsorbent showed good reusability up to the third cycle. The Cr (III) ion removal percentage decreases as we go from the first cycle to the seventh cycle. This reduction could be due to two causes. First, during the recovery step of adsorbents, loss of materials (for instance, carbon) may exist, which decreases the adsorbent amount and materials needed to adsorb dyes for the next cycle. Hence, the adsorbent recovery will not be complete. Second, during recovery steps, adsorbents might have changes in their properties, such as fouling and aggregation. Reduction of surface area and active sites might also occur due to the irreversible particle aggregation during the reusing cycles.

Table 5: Adsorption isotherm.

Langmuir isotherm parameters				Freundlich isotherm parameters			
Equation	R^2	q_m (mg/g)	K_L (L/g)	Equation	R^2	K_F (L/g)	$1/n$
$Y = 89.1X + 11.4$	0.87	0.011	7.82	$Y = 1.1X - 0.99$	0.88	0.37	0.92

Table 6: Adsorption kinetics.

Pseudo-first order				Pseudo-second order			
Equation	R^2	q_e (mg/g)	K_1 (min^{-1})	Equation	R^2	K_2 ($g \cdot mg^{-1} \cdot min$)	q_e (mg/g)
$Y = -7.81X + 1.67$	0.99	$10^{-7.81}$	3.85	$Y = 0.0183X + 1.14$	0.98	2.94×10^{-4}	54.65

Table 7: Comparison of this research with other research.

Precursor material	Qe max (mg/g)	Activating agent	BET surface area (m^2/g)	References
Sugar industrial waste	41.20	—	520.6	[47]
Mango kernel	7.80	H_3PO_4	490.4	[48]
Cashew nut shells	13.93	KOH	1120	[49]
Groundnut shell activated carbon embedded with aluminum metal	13.45	Blending with Al	—	[50]
Waste lignocellulosic material (*Ziziphus jujuba* cores)	96.00	Rubidium carbonate	608.31	[51]
Flamboyant (*Delonix regia*) pod	16.13	H_2SO_4	—	[52]
Agricultural waste material	10.97	H_2SO_4	512	[53]
Olive-mill waste	18.76	KOH	1641	[54]
Macadamia nut shell-derived activated carbon and attapulgite clay combination	96.28	Mixing in 1 : 1 ratio	689	[55]
Cordia africana	54.65	Phosphoric acid	700	This paper

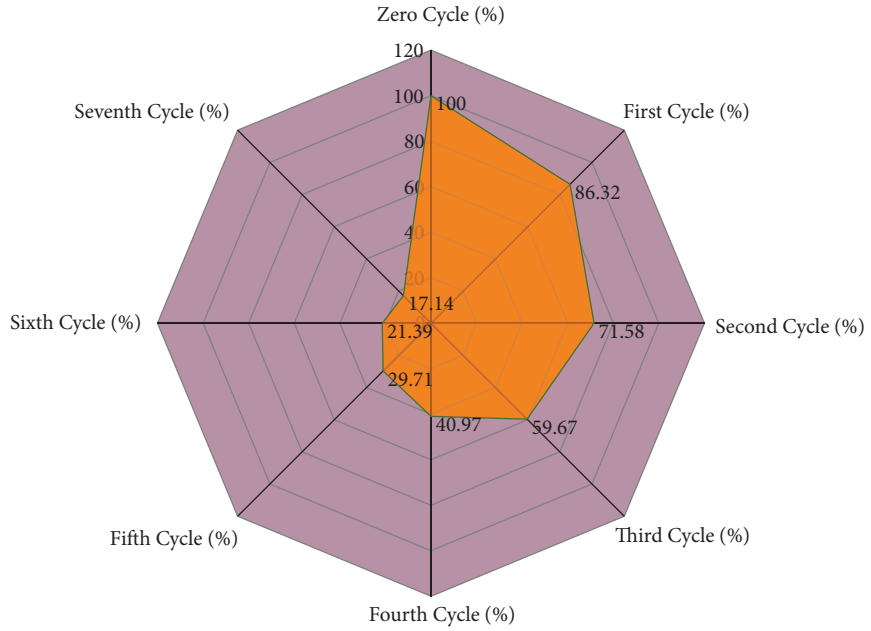

Figure 7: Regeneration study.

4. Conclusions

The synthesis of activated carbon derived from the leaves of *Cordia africana* was optimized using phosphorus acid concentration and activation temperature. Yield and surface area were response variables. The high yield (67%) and surface area (700 m^2/g) were attained at an acid concentration of 85% and activation temperature of 500°C. From proximate analysis, the low moisture content, ash content, and high fixed carbon indicate that the prepared activated carbon has good adsorbent characteristics. Maximum Cr (III) removal was attained at a contact time of 180 min,

adsorbent dose of 1.5 g, initial concentration of 0.6 g/L, and mixing speed of 300 rpm. The equilibrium data were best fitted with Freundlich isotherm with an R^2 value of 0.88, which indicates that the adsorption process was conducted on a heterogeneous surface and adsorption capacity is related to the concentration of the adsorbent. The pseudo-first-order kinetics model with an R^2 value of 0.99 best fits the equilibrium data, which indicates that physisorption controls the adsorption kinetics. In the regeneration study, the Cr (III) ion removal percentage decreases as we go from the first cycle to the seventh cycle. The adsorbent showed good reusability up to the third cycle. Generally, it can be concluded that the activated carbon derived from the leaves of *Cordia africana* showed promising results to be used as a low-cost, locally available, and effective adsorbent for the removal of Cr (III) from wastewater. However, further investigation of the precursor is still needed before its application at industrial level [56].

Data Availability

The data used to support the findings of this study are included within the article.

Conflicts of Interest

The authors declare that they have no conflicts of interest.

Authors' Contributions

All the authors made significant contributions to the manuscript and agreed to its publication.

Acknowledgments

We would like to thank Addis Ababa Science and Technology University (AASTU) and the University of South Africa (UINSA) for providing us with support and laboratory facilities.

References

[1] G. Y. Abate, A. N. Alene, A. T. Habte, and D. M. Getahun, "Adsorptive removal of malachite green dye from aqueous solution onto activated carbon of catha edulis stem as a low cost bio-adsorbent," *Environmental Systems Research*, vol. 9, no. 1, pp. 29–13, 2020.

[2] A. Alemu, B. Lemma, and N. Gabbiye, "Adsorption of chromium (III) from aqueous solution using vesicular basalt rock," *Cogent Environmental Science*, vol. 5, no. 1, Article ID 1650416, 2019.

[3] K. Sabrina, T. Avellán, I. Bärlund et al., "Capacity challenges in water quality monitoring: understanding the role of human development," *Environmental Monitoring and Assessment*, vol. 192, no. 5, pp. 1–16, 2020.

[4] M. G. Arellano-Sánchez, C. Devouge-Boyer, M. Hubert-Roux, C. Afonso, and M. Mignot, "Quantitative extraction of chromium VI and III from tanned leather: a comparative study of pretreatment methods," *Journal of Leather Science and Engineering*, vol. 3, no. 1, pp. 30–13, 2021.

[5] M. Mia, S. Abu, F. Ahmad, and M. Rahman, "An overview of chromium removal techniques from tannery effluent," *Applied Water Science*, vol. 10, no. 9, pp. 1–22, 2020.

[6] G. Boldrini, C. Sgarlata, I. Lancellotti et al., "Efficient chemical stabilization of tannery wastewater pollutants in a single step process: geopolymerization," *Sustainable Environment Research*, vol. 31, no. 1, pp. 33–11, 2021.

[7] N. A. A. Qasem, R. H. Mohammed, D. U. Lawal, and D. U. Lawal, "Removal of heavy metal ions from wastewater: a comprehensive and critical review," *NPJ Clean Water*, vol. 4, no. 1, pp. 36–15, 2021.

[8] T. A. Aragaw and F. M. Bogale, "Biomass-based adsorbents for removal of dyes from wastewater: a review," *Frontiers in Environmental Science*, vol. 9, 2021.

[9] T. Engida et al., *An Overview of Water Pollution Status in Ethiopia with a Particular Emphasis on Akaki River:A Review*, vol. 3, 2020.

[10] D. Bedada, K. Angassa, A. Tiruneh, H. Kloos, and J. Fito, "Chromium removal from tannery wastewater through activated carbon produced from parthenium hysterophorus weed," *Energy, Ecology and Environment*, vol. 5, no. 3, pp. 184–195, 2020.

[11] A. Medhat, H. H. El-Maghrabi, A. Abdelghany et al., "Efficiently activated carbons from corn cob for methylene blue adsorption," *Applied Surface Science Advances*, vol. 3, Article ID 100037, 2021.

[12] A. R. Lucaci, D. Bulgariu, I. Ahmad, G. Lisa, A. M. Mocanu, and L. Bulgariu, "Potential use of biochar from variouswaste biomass as biosorbent in Co(II) removal processes," *Water (Switzerland)*, vol. 11, no. 8, p. 1565, 2019.

[13] M. A. Naeem, M. Imran, M. Amjad et al., "Batch and column scale removal of cadmium from water using raw and acid activated wheat straw biochar," *Water (Switzerland)*, vol. 11, no. 7, pp. 1–17, 2019.

[14] Md S. Reza, C. S. Yun, S. Afroze et al., "Preparation of activated carbon from biomass and its' applications in water and gas purification, a review," *Arab Journal of Basic and Applied Sciences*, vol. 27, no. 1, pp. 208–238, 2020.

[15] A. Tebeje, Z. Worku, T. T. I. Nkambule, and J. Fito, "Adsorption of chemical oxygen demand from textile industrial wastewater through locally prepared bentonite adsorbent," *International journal of Environmental Science and Technology*, vol. 19, no. 3, pp. 1893–1906, 2021.

[16] E. Vunain, J. B. Njewa, T. T. Biswick, and A. K. Ipadeola, "Adsorption of chromium ions from tannery effluents onto activated carbon prepared from rice husk and potato peel by H3PO4 activation," *Applied Water Science*, vol. 11, no. 9, pp. 1–14, 2021.

[17] Lu Zhou, Y. Liu, S. Liu et al., "Investigation of the adsorption-reduction mechanisms of hexavalent chromium by ramie biochars of different pyrolytic temperatures," *Bioresource Technology*, vol. 218, pp. 351–359, 2016.

[18] J. U. Ani, K. G. Akpomie, U. C. Okoro, L. E. Aneke, O. D. Onukwuli, and O. T. Ujam, "Potentials of activated carbon produced from biomass materials for sequestration of dyes, heavy metals, and crude oil components from aqueous environment," *Applied Water Science*, vol. 10, no. 2, pp. 69–11, 2020.

[19] A. Derero, G. Tesfaye, and Z. Woldemariam, "Variation in seed traits and seedling vigour of Cordia Africana lam. Provenances in Ethiopia," *Journal of Forestry Research*, vol. 28, no. 5, pp. 925–933, 2017.

[20] A. P. G. M. V. Samaraweera, N. Priyantha, W. S. S. Gunathilake, P. A. Kotabewatta, and T. P. K. Kulasooriya, "Biosorption of Cr

(III) and Cr (VI) species on NaOH-modified peel of Artocarpus Nobilis fruit. 1. Investigation of kinetics," *Applied Water Science*, vol. 10, no. 5, pp. 1–11, 2020.

[21] J. Fito, S. Abrham, and K. Angassa, "Adsorption of methylene blue from textile industrial wastewater onto activated carbon of parthenium hysterophorus," *International Journal of Environmental Research*, vol. 14, no. 5, pp. 501–511, 2020.

[22] R. Dhahri, M. Yilmaz, L. Mechi et al., "Optimization of the preparation of activated carbon from prickly pear seed cake for the removal of lead and cadmium ions from aqueous solution," *Sustainability*, vol. 14, no. 6, p. 3245, 2022.

[23] T. K. Trinh, T. Tsubota, S. Takahashi, N. T. Mai, M. N. Nguyen, and N. H. Nguyen, "Carbonization and H 3 PO 4 activation of fern dicranopteris linearis and electrochemical properties for electric double layer capacitor electrode," *Scientific Reports*, vol. 10, no. 1, pp. 1–10, 2020.

[24] A. Yosef, A. T. Adugna, M. Kamaraj, and S. M. Beyan, "Adsorption phenomenon of arundinaria alpina stem-based activated carbon for the removal of lead from aqueous solution," *Journal of Chemistry*, vol. 2021, Article ID 5554353, 9 pages, 2021.

[25] Y. Birhanu, S. Leta, and G. Adam, "Removal of chromium from synthetic wastewater by adsorption onto Ethiopian low-cost odaracha adsorbent," *Applied Water Science*, vol. 10, no. 11, pp. 1–11, 2020.

[26] J. D. Castro-Castro, I. F. Macías-Quiroga, G. I. Giraldo-Gómez, N. R. Sanabria-González, and N. R. Sanabria-González, "Adsorption of Cr (VI) in aqueous solution using a surfactant-modified bentonite," *The Scientific World Journal*, vol. 2020, pp. 1–9, 2020.

[27] K. N. S. Budhiary and I. Sumantri, "Langmuir and Freundlich isotherm adsorption using activated charcoal from banana peel to reduce total suspended solid (TSS) levels in tofu industry liquid waste," *IOP Conference Series: Materials Science and Engineering*, vol. 1053, no. (1), Article ID 12113, 2021.

[28] V. Veeramani, R. Madhu, S. M. Chen, B. S. Lou, J. Palanisamy, and V. S. Vasantha, "Biomass-derived functional porous carbons as novel electrode material for the practical detection of biomolecules in human serum and snail hemolymph," *Scientific Reports*, vol. 5, no. 1, pp. 10141–10149, 2015.

[29] M. Zięzio, B. Charmas, K. Jedynak, M. Hawryluk, and K. Kucio, "Preparation and characterization of activated carbons obtained from the waste materials impregnated with phosphoric acid (V)," *Applied Nanoscience*, vol. 10, no. 12, pp. 4703–4716, 2020.

[30] I. Moulefera, F. J. Garcia-Mateos, A. Benyoucef, J. M. Rosas, J. Rodriguez-Mirasol, and T. Cordero, "Effect of Co-solution of carbon precursor and activating agent on the textural properties of highly porous activated carbon obtained by chemical activation of lignin with H3PO4," *Frontiers in Materials*, vol. 7, p. 153, 2020.

[31] C. I. Contescu, S. Adhikari, N. Gallego, N. Evans, and B. Biss, "Activated carbons derived from high-temperature pyrolysis of lignocellulosic biomass," *Chimia*, vol. 4, no. 3, p. 51, 2018.

[32] K. Phothong, C. Tangsathitkulchai, and P. Lawtae, "The analysis of pore development and formation of surface functional groups in bamboo-based activated carbon during CO2 activation," *Molecules*, vol. 26, no. 18, p. 5641, 2021.

[33] T. S. Tessema, A. T. Adugna, and M. Kamaraj, "Removal of Pb (II) from synthetic solution and paint industry wastewater using activated carbon derived from african arrowroot (canna indica) stem," *Advances in Materials Science and Engineering*, vol. 2020, pp. 1–10, 2020.

[34] M. D. G. de Luna, E. D. Flores, D. A. D. Genuino, C. M. Futalan, and M. W. Wan, "Adsorption of eriochrome black T (EBT) dye using activated carbon prepared from waste rice hulls—optimization, isotherm and kinetic studies," *Journal of the Taiwan Institute of Chemical Engineers*, vol. 44, no. 4, pp. 646–653, 2013.

[35] H. Xiao, H. Peng, S. Deng, X. Yang, Y. Zhang, and Y. Li, "Preparation of activated carbon from edible fungi residue by microwave assisted K2CO3 activation—application in reactive black 5 adsorption from aqueous solution," *Bioresource Technology*, vol. 111, pp. 127–133, 2012.

[36] T. Mkungunugwa, S. Manhokwe, A. Chawafambira, and M. Shumba, "Synthesis and characterisation of activated carbon obtained from marula (sclerocarya birrea) nutshell," *Journal of Chemistry*, vol. 2021, pp. 1–9, 2021.

[37] B. Kaźmierczak, J. Molenda, and M. Swat, "The adsorption of chromium (III) ions from water solutions on biocarbons obtained from plant waste," *Environmental Technology & Innovation*, vol. 23, Article ID 101737, 2021.

[38] S. Gogoi, S. Chakraborty, and M. Dutta Saikia, "Surface modified pineapple crown leaf for adsorption of Cr (VI) and Cr (III) ions from aqueous solution," *Journal of Environmental Chemical Engineering*, vol. 6, no. 2, pp. 2492–2501, 2018.

[39] D. Saad, "Selective removal of Cr (III) from aqueous solution using cross-linked polyethylenimine: experimental optimization and modeling," *Polymer Bulletin*, vol. 79, no. 3, pp. 1583–1595, 2021.

[40] R. R. Karri, J. N. Sahu, and B. C. Meikap, "Improving efficacy of Cr (VI) adsorption process on sustainable adsorbent derived from waste biomass (sugarcane bagasse) with help of ant colony optimization," *Industrial Crops and Products*, vol. 143, Article ID 111927, 2020.

[41] T. S. Badessa, E. Wakuma, A. M. Yimer, and A. M. Yimer, "Bio-sorption for effective removal of chromium (VI) from wastewater using moringa stenopetala seed powder (MSSP) and banana peel powder (BPP)," *BMC chemistry*, vol. 14, no. 1, pp. 71–12, 2020.

[42] A. S. Yusuff, "Adsorption of hexavalent chromium from aqueous solution by Leucaena Leucocephala seed pod activated carbon: equilibrium, kinetic and thermodynamic studies," *Arab journal of basic and applied sciences*, vol. 26, no. 1, pp. 89–102, 2019.

[43] C. C. Timbo, M. Kandawa-Schulz, M. Amuanyena, and H. M. Kwaambwa, "Adsorptive removal from aqueous solution of Cr (VI) by green moringa tea leaves biomass," *Journal of Encapsulation and Adsorption Sciences*, vol. 07, no. 02, pp. 108–119, 2017.

[44] J. D. Castro-Castro, N. R. Sanabria-González, G. I. Giraldo-Gómez, and G. I. Giraldo-Gómez, "Experimental data of adsorption of Cr (III) from aqueous solution using a bentonite: optimization by response surface methodology," *Data in Brief*, vol. 28, Article ID 105022, 2020.

[45] L. Liang, J. Wang, X. Tong, and S. Zhang, "Enhanced adsorptive removal of Cr (III) from the complex solution by NTA-modified magnetic mesoporous microspheres," *Environmental Science and Pollution Research*, vol. 29, no. 30, pp. 45623–45634, 2022.

[46] K. L. Tan and B. H. Hameed, "Insight into the adsorption kinetics models for the removal of contaminants from aqueous solutions," *Journal of the Taiwan Institute of Chemical Engineers*, vol. 74, pp. 25–48, 2017.

[47] N. F. Fahim, B. Barsoum, A. Eid, and M. Khalil, "Removal of chromium (III) from tannery wastewater using activated

carbon from sugar industrial waste," *Journal of Hazardous Materials*, vol. 136, no. 2, pp. 303–309, 2006.

[48] M. K. Rai, G. Shahi, V. Meena et al., "Removal of hexavalent chromium Cr (VI) using activated carbon prepared from mango kernel activated with H3PO4," *Resource-efficient technologies*, vol. 2, pp. S63–S70, 2016.

[49] S. Tangjuank, N. Insuk, V. Udeye, and J. Tontrakoon, "Chromium (III) sorption from aqueous solutions using activated carbon prepared from cashew nut shells," *International Journal of the Physical Sciences*, vol. 4, no. 8, pp. 412–417, 2009.

[50] D. R. Vaddi, T. R. Gurugubelli, R. Koutavarapu, D. Y. Lee, and J. Shim, "Bio-stimulated adsorption of Cr (VI) from aqueous solution by groundnut shell activated carbon@ Al embedded material," *Catalysts*, vol. 12, no. 3, p. 290, 2022.

[51] R. Labied, O. Benturki, A. Y. Eddine Hamitouche, and A. Donnot, "Adsorption of hexavalent chromium by activated carbon obtained from a waste lignocellulosic material (ziziphus jujuba cores): kinetic, equilibrium, and thermodynamic study," *Adsorption Science and Technology*, vol. 36, no. 3–4, pp. 1066–1099, 2018.

[52] S. I. Mustapha, L. Adewoye, F. Aderibigbe, M. Alhaji, M. Adekola, and I Tijani, "Removal of lead and chromium from aqueous solution onto flamboyant (<i>Delonix regia) pod activated carbon," *Nigerian Journal of Technological Development*, vol. 14, no. 2, pp. 56–66, 2018.

[53] D. Mohan, K. P. Singh, and V. K. Singh, "Trivalent chromium removal from wastewater using low cost activated carbon derived from agricultural waste material and activated carbon fabric cloth," *Journal of Hazardous Materials*, vol. 135, no. 1–3, pp. 280–295, 2006.

[54] M. I. Bautista-Toledo, J. Rivera-Utrilla, R. Ocampo-Perez, F. Carrasco-Marin, and M. Sanchez-Polo, "Cooperative adsorption of bisphenol-A and chromium (III) ions from water on activated carbons prepared from olive-mill waste," *Carbon*, vol. 73, pp. 338–350, 2014.

[55] L. Hlungwane, E. L. Viljoen, and V. E. Pakade, "Macadamia nutshells-derived activated carbon and attapulgite clay combination for synergistic removal of Cr (VI) and Cr (III)," *Adsorption Science and Technology*, vol. 36, no. 1–2, pp. 713–731, 2018.

[56] Y. Asrat, A. T. Adugna, M. Kamaraj, and S. M. Beyan, "Adsorption phenomenon of arundinaria alpina stem-based activated carbon for the removal of lead from aqueous solution," *Journal of Chemistry*, vol. 2021, pp. 1–9, 2021.